# Improvement of Image Quality in Transmission Computed Tomography Using Synchrotron Monochromatic X-Ray Sheet Beam

T. Yuasa[1], T. Takeda[2], T. Zeniya[1], Y. Hasegawa[1], K. Hyodo[3], Y. Hiranaka[1], Y. Itai[2], and T. Akatsuka[1]

[1]Faculty of Engineering, Yamagata Univ., Yonezawa, Japan
[2]Institute of Clinical Medicine, Univ. of Tsukuba, Tsukuba, Japan
[3]Institute of Materials Structure Science, KEK, Tsukuba, Japan
E-Mail: yuasa@eat72.yz.yamagata-u.ac.jp

*Abstract*-**In the transmission CT imaging system with scintillator-CCD detector using synchrotron monochromatic x-ray as sheet beam, improvement of reconstructed image quality is investigated. The properties of experimental facilities cause the incident beam intensity to be spatially inhomogeneous, and to temporally attenuate. In order to achieve more reliable reconstruction, we propose the data-correction and estimation method based on the properties of the facilities and the principle of CT reconstruction, and confirm its effectiveness using a physical phantom.**

## I. INTRODUCTION

Synchrotron radiation (SR) attracts researchers in biomedical imaging field because of its excellent properties such as broad and continuous spectrum, high brilliance, and high directionality. From the properties, SR provides much higher-quality monochromatic x-ray beam with high brilliance and directionality than the conventional x-ray tube, and then releases the difficulty in imaging by x-ray tube, *e.g.*, beam hardening effects causing degradation of image qualities [1-14]. To obtain high contrast CT images, there is introduced a highly sensitive imaging system using scintillator-CCD detector system by incident sheet beam, which drastically reduces data-acquisition time compared with pencil beam, while sheet-beam-used imaging slightly degrades image qualities due to scattered x-rays [7, 8, 12, 13, 14]. In spite of using both the high-quality x-ray source and the highly sensitive imaging system, the reconstructed image quality is degraded because of the following reasons: First, the intensity profile of incident sheet beam represents spatial inhomogeneity. Second, the intensity of incident beam temporally attenuates in the course of measurements due to the properties of experimental facilities. The fact reveals that high quality SR-imaging requires not only highly sensitive imaging system but also reliable data estimation based on the properties of the experimental facilities. In this research, we propose the data-estimation and correction method for SR-imaging with incident sheet beam, and demonstrate its effectiveness using a physical phantom.

## II. TRANSMISSION X-RAY CT IMAGING SYSTEM BY INCIDENT SHEET BEAM

Fig. 1 shows the constitution of transmission CT imaging system by incident x-ray sheet beam [7, 14]. Incident white x-ray beam from the accelerator is monochromated with the Si (111) double-crystal Bragg-Bragg monochromator. Then, the object on the rotational scanning stage is irradiated with the beam collimated to $2 \times 40$ mm$^2$ rectangular intensity profile using the tantalum slit. The transmitted x-ray is converted to visible light by the scintillating screen for medical purposes (HR-6, FUJI FILM), which is detected with the CCD camera (CCD15-11, Astro Cam) after being reflected by the mirror and focused by the lens. The CCD and the rotational stage are controlled by PC. The optical system from the scintillating screen to the CCD is covered with black sheet to avoid strayed light, and the CCD is set at right angle against the incident beam to avoid the direct x-ray irradiation, and detects signal light as 2-D data with 16-bit gray scale, whose pixel size and image size are $181 \times 181$ μm$^2$, and $1024 \times 256$ pixels, respectively. The system was constructed at bending magnet beam line NE-5A of the Tristan Accumulation Ring (6.5 GeV, 10-40 mA) in KEK, Japan. Fig. 2 shows an example of measured 2-D data without an object and its vertical and horizontal profiles. Projection data was generated from the 2-D image data from the CCD as follows: First, irradiated region is extracted by the thresholding method, and next the datum in a bin is generated by summing pixel-values of adjacent 12 and 10 pixels in vertical and horizontal directions, respectively, for reducing statistical noise. Thereby, projection data were obtained.
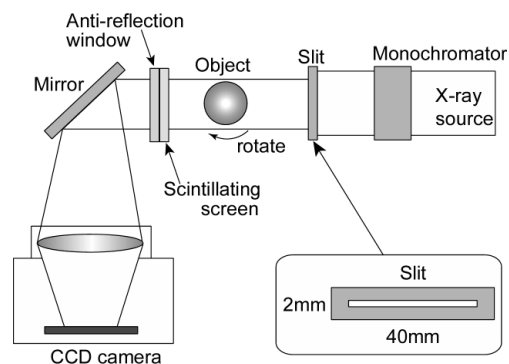


Fig. 1. Schematic of tansmission x-ray computed tomography imaging system using synchrotron monochromatic x-ray sheet beam.

## III. CORRECTION FOR SPATIAL INHOMOGENEITY IN INCIDENT BEAM INTENSITY

Fig. 3 shows a projection without an object obtained from the data of Fig. 2. One can see the spatial inhomogeneity of incident

# Report Documentation Page

| Report Date 25OCT2001 | Report Type N/A | Dates Covered (from... to) - |
|---|---|---|

| | |
|---|---|
| **Title and Subtitle** Improvement of Image Quality in Transmission Computed Tomography Using Synchrotron Monochromatic X-Ray Sheet Beam | **Contract Number** |
| | **Grant Number** |
| | **Program Element Number** |
| **Author(s)** | **Project Number** |
| | **Task Number** |
| | **Work Unit Number** |
| **Performing Organization Name(s) and Address(es)** Faculty of Engineering, Yamagata Univ., Yonezawa, Japan | **Performing Organization Report Number** |
| **Sponsoring/Monitoring Agency Name(s) and Address(es)** US Army Research, Development & Standardization Group (UK) PSC 802 Box 15 FPO AE 0949-1500 | **Sponsor/Monitor's Acronym(s)** |
| | **Sponsor/Monitor's Report Number(s)** |

**Distribution/Availability Statement**
Approved for public release, distribution unlimited

**Supplementary Notes**
Papers from the 23rd Annual International Conference of the IEEE Engineering in Medicine and Biology Society, October 25-28, 2001, Istanbul, Turkey. See also ADM001351 for entire conference on cd-rom.

**Abstract**

**Subject Terms**

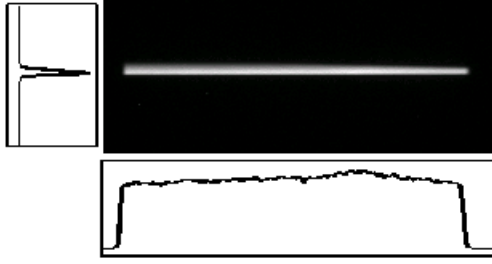| **Report Classification** unclassified | **Classification of this page** unclassified |
|---|---|
| **Classification of Abstract** unclassified | **Limitation of Abstract** UU |

**Number of Pages**
4

Fig. 2. Example of measured incident beam and its vertical and horizontal profiles
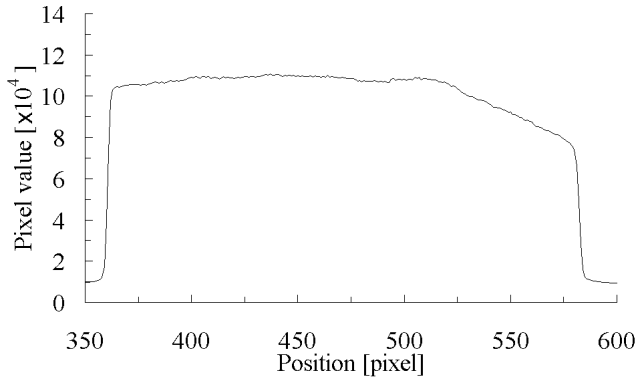


Fig. 3. Example of spatially inhomogeneous indident intensity obtained from the measured data

beam. The causes of the inhomogeneity are as follows: (1) inhomogeneity of sensitivity among pixels of CCD camera, (2) spatial inhomogeneity of incident white beam intensity itself from an accelerator, and (3) monochromator deformed by heat due to incident white beam. For (1), one can easily correct the effect by employing projections obtained from a water-filled cylindrical physical phantom. We do not consider (1) because the effective correction method has been established. For (2), it is very difficult to obtain homogeneous incident beam profile in spite of carefully adjusting it before setting up the system. For (3), although the monochromator is water-cooled to reduce the heat effect, it is impossible to suppress the deformation because of continuous irradiation of white beam with intense intensity. (2) and (3) are proper to synchrotron radiation facilities.

Since the homogeneities in incident beam intensity caused by (2) and (3) depend on the status of experimental facilities when imaging, correction method must reflect the status. So, we paid attention to an intensity profile obtained just before imaging an object. Let $i(r)$, $t(r, \theta)$, and $t'(r, \theta)$ be an intensity profile of incident beam obtained just before measurements, a measured transmission profile at projection angle $\theta$, and its corrected transmission profile, respectively, where $r$ and $\theta$ are defined as shown in Fig. 4. Assuming that the spatial inhomogeneity does not change in the course of measurements, one can estimate the transmission profile $t'(r, \theta)$ obtained when imaging the object with spatially homogeneous sheet-beam by normalizing the measured transmission profile $t(r, \theta)$ with an intensity profile $i(r)$ as

$$t'(r, \theta) = t(r, \theta) i_0 / i(r), \qquad (1)$$

where $i_0$ is a spatial average value of $i(r)$.

## IV. Correction for temporal attenuation in incident beam intensity

With a decrease in the number of electrons in the accelerator ring the synchrotron radiation beam intensity gradually decreases proportionally to the electron number. Fig. 5 shows the temporal attenuation of projection data obtained from a physical phantom. One way in which one detects the intensity attenuation is a ring current value proportional to the number of electrons in the ring. In fact, so far we have employed the ring current data to correct the intensity attenuation. However, although the ring current is highly correlated with the beam intensity, there does not exist the strictly quantitative relationship between them. Thus, it is insufficient for a correction parameter. Another way is to monitor the attenuation with an ion chamber set on the upper-stream side than the object. However, although the method is effective for measurements with pencil beam, it is not suitable to measurements with sheet beam because an ion chamber can not acquire a spatial information of the beam.

First, we pay attention to the fact that total X-ray quantity absorbed in the object is constant when imaging with the spatially homogeneous incident sheet beam independently of projection angle $\theta$. In fact, letting $f(x, y)$ be the spatial distribution of the linear attenuation coefficients, the projection for projection angle $\theta$ is given as
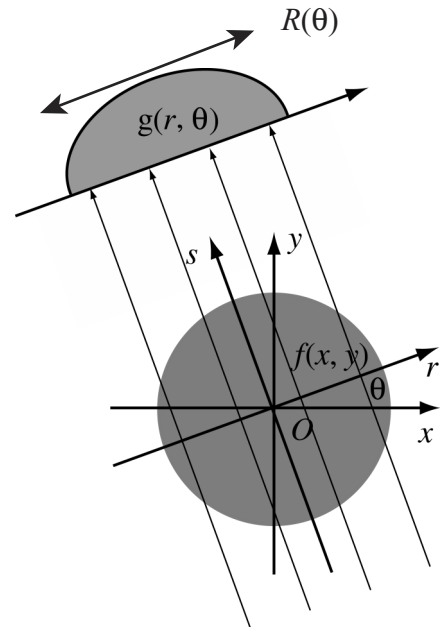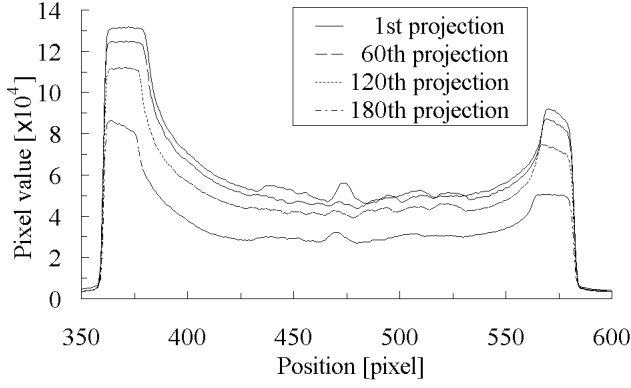


Fig. 4. Coordinate system of CT

Fig. 5. Example of temporal attenuation of transmitted x-ray intensity

$$g(r,\theta)$$
$$= \int_{-\infty}^{+\infty} f(r\cos\theta - s\sin\theta, r\sin\theta - s\cos\theta)ds. \qquad (2)$$

Accordingly, the above-mentioned fact can be easily proved as follows:

$$g(r,\theta)$$
$$= \int\int_{-\infty}^{+\infty} f(r\cos\theta - s\sin\theta, r\sin\theta - s\cos\theta)dsdr$$
$$= \int\int_{-\infty}^{+\infty} f(x,y)dxdy = const., \qquad (3)$$

where the integral interval was set to (-∞, ∞) because $f(x, y)$ is a spatially localized function, and the relationship between coordinate systems, $(x, y)$ and $(s, t)$, was used.

The relationship among the transmission profile corrected for the spatial inhomogeneity $t'(r, \theta)$, the average intensity $i_0$, and the projection $g(r, \theta)$ is given as

$$\log t'(r,\theta) = \log i_0 - g(r,\theta). \qquad (4)$$

Here, note that the corrected intensity $t'(r, \theta)$ is assumed to be obtained using spatially homogeneous incident sheet beam. Integrating with respect to $r$, and then arranging,

$$\int_{R(\theta)} \left(\log t'(r,\theta) - \log i_0\right)dr = -\int_{R(\theta)} g(r,\theta)dr, \qquad (5)$$

where integral interval $R(\theta)$, which depends on projection angle $\theta$, is introduced as shown in Fig. 4 to reduce to the utmost the influence of the inhomogeneity of the region outside the object in the intensity upon the correction. If incident intensity does not temporally decrease, the left hand side of Eq. (5) is constant independently of projection angle $\theta$ from the above fact. Therefore, one should correct the temporal attenuation such that ∫ log $(t'(r, \theta)/i_0)$ d$r$ for each $\theta$ be constant by normalizing it to the value at projection angle $\theta = 0$, ∫ log $(t'(r, 0)/i_0)$ d$r$. Hence, the transmission intensity is corrected as follows:

$$\log t''(r,\theta) = \log(t'(r,\theta)/i_0)$$
$$\times \int_{R(0)} \log(t'(r,0)/i_0)dr / \int_{R(\theta)} \log(t'(r,\theta)/i_0)dr + \log i_0. \quad (6)$$

Fig. 6 shows a result in which the transmission intensities of Fig. 5 are corrected with the proposed method. One can see that the spatial and temporal inhomogeneities are satisfactorily corrected. Finally, the projection data is estimated as follows:

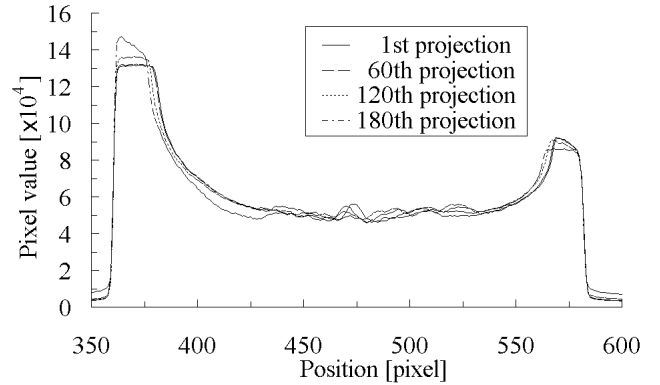$$g'(r,\theta) = \log i_0 - \log t''(r,\theta). \qquad (7)$$



Fig. 6. Profiles of transmission x-ray intensity after correction

## V. EXPERIMENTAL RESULT

Fig. 7 shows the 35-mmφ cylindrical physical phantom made of acrylic which has three channels with diameter of 3, 2, 1.5, and 1 mm, respectively, *i.e.*, totally 12 channels. The incident white x-ray is monochromated to 34.6 keV. The exposure time of CCD detector is 20 ms so as to effectively use its dynamic range. The phantom is imaged over 180 degrees with rotational step of 1 degree, and the image is reconstructed using the filtered backprojection method with the Shepp-Logan filter. Figs. 7 (b), and (c) show the reconstructed images with the ring current, and the proposed corrections, respectively. From the images, one can see that the image with the proposed correction is reconstructed more smoothly than that with the conventional correction based on the ring current value. To confirm the fact, the profile of the reconstructed images on the line passing through the centers of three channels of 1 mmφ is shown in Fig. 8, where the large peak shown in the right region of the profile for the ring current correction is truncated at level 255 for detailed comparison of image contrast. From the figure, one can again see that the acrylic region of the image with the proposed correction is more smooth than that with the ring current correction. Furthermore, one can recognize that the edges of the image with the proposed correction is sharper than that with the ring current correction.
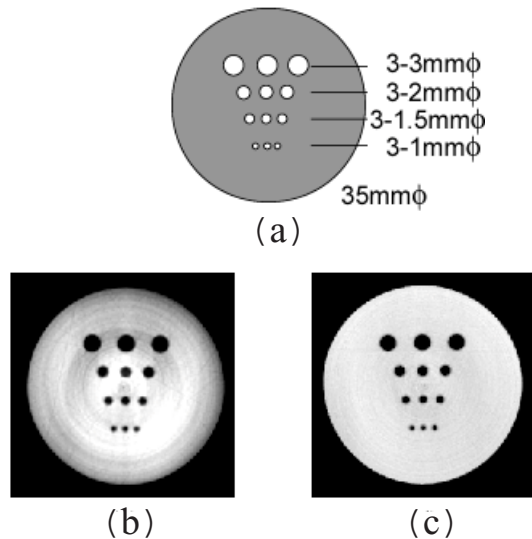
(a)



(b)                              (c)

Fig. 7. Comparison of reconstructed images, (a) Physical phantom, (b) Reconstructed image of the physical phantom with correction by ring current, (c) Reconstructed image of the physical phantom with correction of spatial inhomogeniety and temporal attenuation.
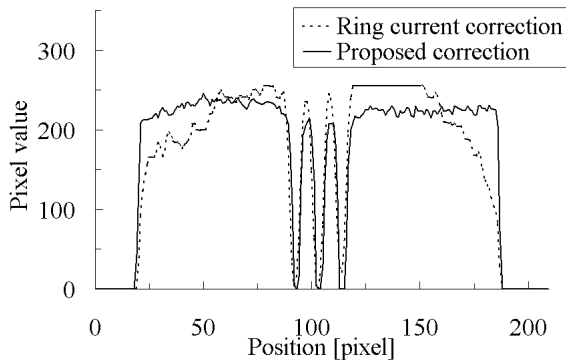


Fig. 8. Horizontal profiles of the reconstructed images of the physical phantom

## V. CONCLUDING REMARKS

In synchrotron monochromatic x-ray sheet beam used transmission CT imaging system with the scintillator-CCD detector, we proposed and investigated the corrections for spatial homogeneity in incident beam intensity by using the incident beam profile obtained just before imaging objects, and for temporal attenuation in incident beam intensity by using the constant value based on the CT principle. As a result, it is indispensable to correct and then estimate the projection data based on the properties of the experimental facilities and the CT reconstruction principle in order to reliably reconstruct images with the excellent abilities of synchrotron radiation as the light source.

However, Fig. 6 shows that the regions outside the object in the 180th estimated projection, where x-rays directly impinge on the detector without passing through the object, are different in shape from those at other projections. This fact represents that the assumption that the incident intensity profile does not change throughout the measurement does not hold. Although we introduced the integral interval $R(\theta)$ to reduce this difficulty, it may be insufficient for more reliable reconstruction. It will be effective to correct projections using two profiles, *i.e.*, the intensity profiles without an object obtained just before and after the measurement, while we used only one profile obtained just before the measurement.

## REFERENCES

[1] J. S. Meyer, L. A. Hayman, L. A. Yamamoto, M. Sasaki, and F. Nakajima, "Local cerebral blood flow measured by CT after stable xenon inhalation," A. J. R., 135, pp. 239-251, 1980.
[2] A. C. Thompson, J. Llacer, C. Finman, E. B. Hughes, J. N. Otis, S. Wilson, and H. D. Zeman,"Computed tomography using synchrotron radiation," Nucl. Instr. Meth., 222, pp. 1208-1213, 1984.
[3] Y. Nagata, H. Yajima, K. Hayashi, K. Kawashima, K. Hyodo, K. Kawata, and M. Ando, "High energy high resolution monochromatic x-ray computed tomography using the Photon Factory vertical wiggler beamline," Rev. Sci. Instr., 63, pp. 615-618, 1992.
[4] T. Hirano, K. Usami, and K. Sakamoto, "High resolution monochromatic tomography with x-ray sensing pickup tube," Rev. Sci. Instr., 60(7), pp. 2482-2485, 1989.
[5] J. H. Kinney, Q. C. Johnson, M. C. Nichols, U. Bonse, R. A. Saroyan, R. Nusshardt, and R. Pahl, "X-ray microtomography on beamline X at SSRL," Rev. Sci. Instr., 60(7), pp. 2471-2474, 1989.
[6] J. H. Kinney, Q. C. Johnson, R. A. Saroyan, U. Bonse, R. Nusshardt, and R. Pahl, "Syndcrotron microtomography of supported catalysts," Rev. Sci. Instr., 60(7), pp. 2475-2478, 1989.
[7] T. Takeda, M. Kazama, T. Zeniya, T. Yuasa, M. Akiba, A. Uchida, K. Hyodo, T. Akatsuka, M. Ando, and Y. Itai, "Development of a Monochromatic X-ray Computed Tomography with Synchrotron Radiation for Functional Imaging," in Medical Applications of Synchrotron Radiation, edited by M. Ando and C. Uyama (Springer-Verlag, Tokyo), pp. 103-110 (1998).
[8] Y. Itai, T. Takeda, T. Akatsuka, T. Maeda, K. Hyodo, A. Uchida, T. Yuasa, M. Kazama, J. Wu, and M. Ando, "High contrast computed tomography with synchrotron radiation," Rev. Sci. Instrum., 66(2), pp. 1385-1387, 1995.
[9] K. Engelke, M. Lohmann, "A system for dual energy microtomography of bones," Nucl. Instr. Meth., A174, pp. 380-389, 1989.
[12] A. Koch, "Lens coupled scintillating screen-CCD X-ray area detector with a high detective quantum efficiency," Nucl. Instr. Meth., A348, pp. 654-658, 1994.
[13] M. Kazama, M. Akiba, T. Takeda, T. Yuasa, K. Hyodo, M. Ando, T. Akatsuka, and Y. Itai, "Performance Study of Monochromatic Synchrotron X-ray Computed Tomography using a Linear Array Detector," Medical Imaging Technology, Vol. 15, No. 5, pp. 615-624, 1997.
[14] A. Hoshino, T. Takeda, M. Akiba, M. Kazama, Y. Watanabe, T. Yuasa, K. Hyodo, A. Uchida, T. Akatsuka, and Y. Itai, "Coherent Scatter Computed Tomography with Scintillator-CCD System," Proc. of Int. Conf. IEEE/EMBS, pp. 627-628, 1996.